

Effects of sodium chloride on the properties of chlorophyll *a* submonolayer adsorbed onto hydrophobic and hydrophilic surfaces using broadband spectroscopy with single-mode integrated optical waveguides

Rodrigo S. Wiederkehr

University of Louisville
Department of Physics and Astronomy
2210 South Brook Street
Louisville, Kentucky 40292

Geoffrey C. Hoops

Butler University
Department of Chemistry
4600 Sunset Avenue
Indianapolis, Indiana 46208

Sergio B. Mendes

University of Louisville
Department of Physics and Astronomy
2210 South Brook Street
Louisville, Kentucky 40292
E-mail: sb.mendes@louisville.edu

Abstract. In this work, we experimentally investigated the effects of sodium chloride on the molar absorptivity and surface density of a submonolayer of chlorophyll *a* adsorbed onto hydrophilic and hydrophobic solid/liquid interfaces. Those investigations were made possible by a broadband spectroscopic platform based on single-mode, integrated optical waveguides, which allows for extremely sensitive spectroscopic detection of analytes immobilized at submonolayer levels. Chlorophyll *a* with a constant bulk concentration (1.4 μM) was dissolved in phosphate buffer solutions (7 mM) of neutral pH, but with different sodium chloride concentrations. For a buffer solution of 1 mM of sodium chloride, the measured surface density of chlorophyll *a* was 0.209 pmol/cm² for a hydrophilic and 0.125 pmol/cm² for a hydrophobic surface. For a phosphate buffer solution of 10 mM of sodium chloride, the measured surface density of chlorophyll *a* was 0.528 pmol/cm² for a hydrophilic and 0.337 pmol/cm² for a hydrophobic surface. Additionally, a hypsochromic shift of the Soret band was observed for the adsorbed pigment in correlation with an increase in buffer ionic strength. The adsorption of chlorophyll *a* onto different surfaces can play an important role to elucidate several processes found in nature and provide a rationale for bio-inspired new material technologies.

© 2011 Society of Photo-Optical Instrumentation Engineers (SPIE). [DOI: 10.1117/1.3564421]

Subject terms: chlorophyll *a*; molecular surface adsorption; waveguide spectroscopy; atomic layer deposition; molecular vapor deposition silane; perfluorodecyltrichlorosilane.

Paper 100893SSR received Oct. 30, 2010; revised manuscript received Feb. 10, 2011; accepted for publication Feb. 15, 2011; published online Apr. 21, 2011.

1 Introduction

Chlorophyll *a* is a key biochemical component in the molecular apparatus that is responsible for photosynthesis, the critical process in which the energy from sunlight is used to produce life-sustaining oxygen. In the photosynthetic reaction sequence, water is oxidized to oxygen^{1,2} and chlorophyll powers this redox chemistry both by absorbing light to attain an excited electronic state and also by transferring this excitation energy to the photosystem reaction centers, where the energy is trapped in a photochemical reaction.^{3–5} Most of the chlorophyll molecules found in nature are bound to a class of photosynthetic proteins, called light harvesting complex,⁶ embedded in the thylakoid membranes of chloroplasts present in plants and algae cells.⁷ The principal chromophore of a chlorophyll *a* molecule is a porphyrin ring, coordinated to a central magnesium metal atom (see Fig. 1). Chlorophyll *a* absorbs light in the visible spectrum at approximately 400 to 440 nm (Soret band) and 660 to 680 nm (Q band). The peak position in both regions strongly depends on the solvent composition surrounding the pigment.^{8,9} Chlorophyll *a* also fluoresces at the 680 to 688 nm spectral region when excited by light with a shorter wavelength (e.g., 435 nm).¹⁰ Those

optical properties from chlorophyll *a* are used for several applications such as the identification of microalgae and phytoplankton in the ocean,^{11,12} the study of reactions occurring at different time scales in plants and algae cells,^{13–15} and recently have been investigated for performance improvement of dye-sensitized thin-film solar cells.^{16,17} In most of these applications, chlorophyll *a* is found in contact with a surface (e.g., cell membranes, thin-film solid surface); however, due to the lack of sensitivity in conventional instrumentation, there are only a few reports in the literature characterizing chlorophyll *a* adsorbed to surfaces at monolayer or submonolayer levels,^{18–21} and none of them consider the combined effect of the solution composition and the surface chemistry on the optical properties of the adsorbed pigment. When a liquid solution comes in contact with a solid surface, several competing forces can eventually drive the surface adsorption of molecules that were originally dissolved in the solution.²² Surface-adsorbed biomolecules will then be exposed to a fairly different nano-environment that may eventually alter the molecular optical properties.²³ The composition of the solvent that is used to dissolve a biomolecule also plays an important role in the adsorption process by altering the affinity of the molecule with the surface.²⁴

Single-mode integrated optical waveguides is a highly sensitive technique for investigation of surface-adsorbed

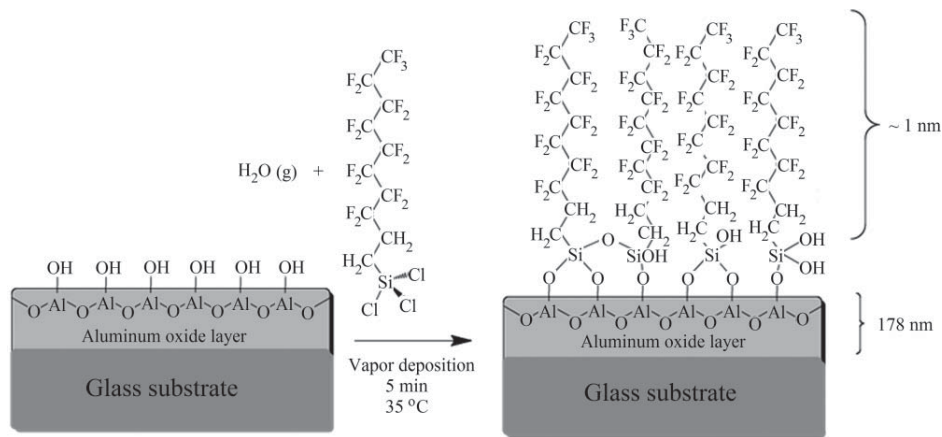


Fig. 4 Hydrophobic functionalization of the aluminum oxide waveguide surface.

in the aqueous solution. However, aqueous solutions of two different concentrations of sodium chloride (1 and 10 mM) were investigated for their impact on the physical/chemical properties of the chlorophyll *a* submonolayer.

2 Experimental Procedures

2.1 Chlorophyll *a* Preparation

Chlorophyll *a* from *anacystis nidulans* algae was commercially obtained (Sigma Aldrich, C6144) and dissolved in a solution of 80% (v/v) acetone (Sigma Aldrich, 650501, Chromasolv plus $\geq 99.9\%$) with 20% de-ionized water (Millipore Direct 3Q water purification system). The initial concentration of chlorophyll *a* in the stock solution was 27.3 μM . To obtain solutions with a final concentration of 1.4 μM of chlorophyll *a*, the stock solution was diluted in 7 mM of sodium phosphate with 1 or 10 mM of sodium chloride ($\text{pH} = 7.25$).

2.2 Optical Waveguide Spectroscopy of Chlorophyll *a*

The single-mode, integrated optical waveguide spectrometer (shown in Fig. 2) for the data acquisition reported in this study was developed in our laboratories and reported in detail elsewhere.^{31,32,35} The setup used is composed of a broadband light source, a single-mode planar optical waveguide with integrated grating couplers, a flowcell, a monochromator, and a charge coupled device (CCD) array detector. The light source used was a tungsten-halogen lamp (Philips, FocusLine) with 4.5 V and 2.55 A. An optical filter (BG 40 from Schott) was placed in front of the light source to limit the spectral content inside the probing region to wavelengths shorter than 650 nm and to prevent the near infrared wavelengths, which are not coupled to the waveguide, from getting inside the flowcell and generating heat and photobleaching of the solution dissolved species.³⁶ To couple broadband light into the single-mode planar integrated optical waveguide, two diffraction gratings (3.4 cm apart from each other) were micro-fabricated into the glass substrate. For this purpose, a photoresist film (Shipley 1805) was photo-patterned by a holographic technique.³⁷ After exposure and development of the holographic pattern, an ion milling dry etching process

with argon and CF_4 as etchants was performed to transfer the periodic modulation present in the photoresist film onto the surface of the glass slide substrate. The periodicity of the fabricated grating couplers was 250 nm and the coupled bandwidth was from 400 nm (due to the spectral limitations on the light source) to 500 nm. The broad spectral bandwidth was achieved by a solid immersion lens device to create a highly anamorphic beam of large numerical aperture, as previously described by our group.³¹ A linear polarizer was placed in the optical path to allow for only the transverse electric (TE) light modes to couple into the waveguide. The outcoupled light beam was fiber-guided to a monochromator (SpectraPro 2300, Princeton Instruments) that dispersed the light beam to a charge coupled device (CCD Pixis 400, Princeton Instruments) with each column in the CCD array corresponding to a specific wavelength.

The glass substrates, each with a pair of integrated grating couplers, were coated with a thin-film of aluminum oxide using an atomic layer deposition tool (Beneq TFS200). The alumina thin-film was chosen as the waveguide material due to its high refractive index and low propagation loss (less than 1 dB/cm) over a broad spectral range, including the violet/blue region of the optical spectrum.³² The precursors used in the atomic layer deposition process for the alumina film were trimethylaluminum and water. These precursors were alternately injected into the deposition chamber to create a self-limiting atomic layer on the glass substrate surface for each complete cycle.^{32,35} The deposition temperature in the reactor chamber was 200°C and the number of cycles to reach the thickness of 178 nm was 1670.

To functionalize the waveguide surface, an organic monolayer was coated over the aluminum oxide layer by molecular vapor deposition (MVDTM, Applied MicroStructures Inc.).³⁸ The deposition was obtained by sequential vapor injection of the precursors to the reaction chamber under vacuum. To obtain a hydrophilic monolayer, the precursors used were methoxy(polyethyleneoxy)propyltrimethoxysilane (PEG silane, Gelest Inc.) and DI water with a reaction time of 15 min (Fig. 3). To obtain a hydrophobic monolayer, the precursors used were heptadecafluoro-1,1,2,2-(tetrahydrodecyl)trichlorosilane (FDTS, Gelest Inc.) and DI water with a reaction time of 5 min (Fig. 4). In both

cases, the temperature of the precursors was kept at 55°C and the reaction chamber temperature was 35°C. Before the deposition of the organic films, a 60-s oxygen-plasma cleaning was performed to remove any organic residue from the alumina surface. The presence of the aluminum oxide layer, compared to metal or polymeric surfaces, improves the stability and durability of the organic films deposited because of the higher density of the reactive hydroxyl groups on the surface of the oxide film.³⁹

The chlorophyll *a* solution was injected into the flowcell with a volume of approximately 2 ml covering the waveguide surface. All the data acquisition was performed at room temperature (25°C).

2.3 Absorbance Spectra of Chlorophyll *a* in Solution and Surface

The concentration of chlorophyll *a* in solution was obtained by measuring the absorbance at the Q band (672 nm) in solution with a conventional spectrophotometer (Cary 300, Varian). The molar absorptivity of chlorophyll *a* in solution is well known ($\epsilon_{672} = 73,265 \text{ M}^{-1} \text{ cm}^{-1}$).⁴⁰ To ensure that the chlorophyll *a* concentration remained unaltered during our experiment, the sample to be measured was collected after the passage through the waveguide flowcell. Figure 5 shows the absorbance spectra obtained for the solutions with the same buffer pH and chlorophyll *a* concentration, but different concentrations of NaCl; as expected they exhibit a good agreement with each other.

To obtain the absorbance spectra of chlorophyll *a* that were surface-adsorbed onto the functionalized waveguide surface, the integration time for data acquisition in the CCD was fixed at 60 s. The sequence of data collection was the following: first, the buffer solution (without chlorophyll *a*) was injected into the flowcell and a reference signal was acquired; next, the chlorophyll *a* solution was introduced into the flowcell and data was sequentially acquired every 10 min until equilibrium in the amount of surface-adsorbed chlorophyll *a* was reached. A dark current signal was finally acquired by blocking the input light beam.

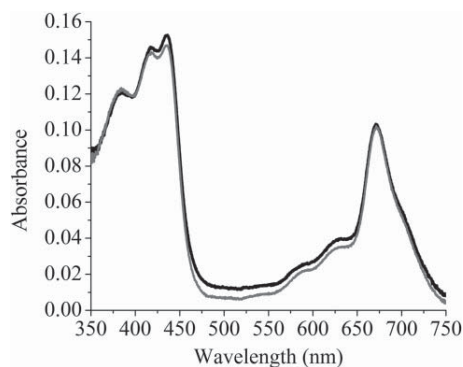


Fig. 5 Absorbance spectra for 1.4 μM of chlorophyll in solutions of different ionic strength. The black curve is chlorophyll *a* dissolved in 7 mM sodium phosphate plus 10 mM of sodium chloride, pH 7.25. The gray curve is chlorophyll *a* dissolved in 7 mM sodium phosphate plus 1 mM of sodium chloride, pH 7.25. The different concentration of sodium chloride does not markedly affect the absorbance of chlorophyll *a* in solution.

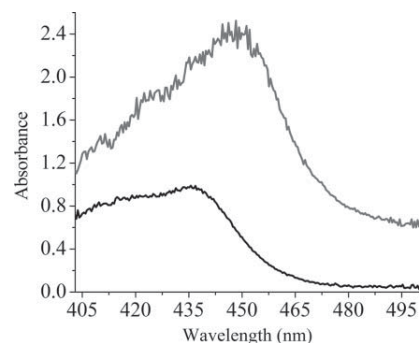


Fig. 6 Absorbance spectra of chlorophyll *a* adsorbed to a hydrophilic surface, acquired after adsorption equilibrium was reached. In both spectra, the amount of chlorophyll *a* dissolved in solution was the same (1.4 μM), as was the pH of the 7 mM sodium phosphate buffer (7.25). Black shows that the concentration of NaCl was 1 mM; gray shows that the concentration of NaCl was 10 mM.

3 Results and Discussions

3.1 Absorbance Measurements of Chlorophyll *a* Adsorbed to Chemically Modified Waveguide Surfaces

The absorbance data for surface-adsorbed chlorophyll *a* are presented in Fig. 6 for the aluminum oxide waveguide functionalized with a hydrophilic surface, and in Fig. 7 for the hydrophobic surface. In all cases, the solution concentration of chlorophyll *a* injected into the flowcell was held constant, but the sodium chloride concentration was varied at two different levels: 1 and 10 mM. The spectra presented in Figs. 6 and 7 correspond to the situation where equilibrium had been reached for the surface-adsorbed species, i.e., enough time had elapsed that no further changes in the spectra were observed. From these data we qualitatively observed that chlorophyll *a* adsorbs to a higher degree to the hydrophilic surface. In order to quantitatively describe the surface density, the sensitivity of the waveguide spectrometer had to be considered.

3.2 Sensitivity of the Waveguide Spectrometer

The sensitivity factor, S , which is defined as the ratio between the absorbance measured using a waveguide platform, A_{WG} ,

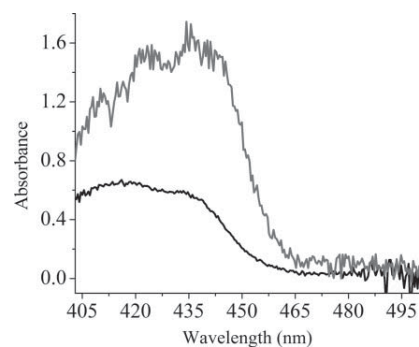


Fig. 7 Spectra of chlorophyll *a* adsorbed to a hydrophobic functionalized surface, acquired after the steady state was reached. In both spectra, the amount of chlorophyll *a* dissolved in solution was the same (1.4 μM), as was the pH of the 7 mM sodium phosphate buffer (7.25). Black shows that the concentration of NaCl was 1 mM; gray shows that the concentration of NaCl was 10 mM.

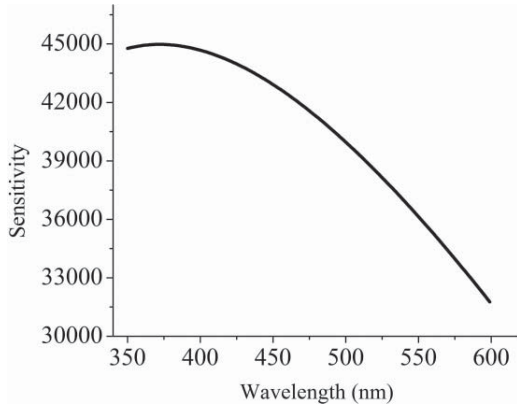


Fig. 8 Sensitivity values calculated for a single-mode waveguide with 178 nm of thickness and considering the following values for the constants: $L = 3.4$ cm, $n_c = 1.33$, with the approximation that $n_l \approx n_c$, $n_s = 1.51$. The effective refractive index, N_{TE} , and the effective thickness, $t_{eff,TE}$, were calculated from the waveguide dispersion equation. The refractive index of the alumina film was calculated using the relation $n_w(\lambda) = a + b/\lambda^2 + c/\lambda^4$, where $a = 1.64576$, $b = 42.89898$, and $c = 308958233.142$ from Ref. 32.

and the absorbance measured in direct transmission, A_{TR} , for an arbitrary layer of chromophores in both cases, is given by^{26,30}

$$S = \frac{A_{WG}}{A_{TR}} = \frac{A_{WG}}{\epsilon_{surf}\Gamma}, \quad (1)$$

where ϵ_{surf} is the molar absorptivity of the surface-bound chromophore and Γ is the chromophore surface density. The sensitivity factor is polarization-dependent and is given by the following expression for the TE-polarization:²⁶

$$S_{TE} = \frac{2n_l(n_w^2 - N_{TE}^2)L}{N_{TE}(n_w^2 - n_c^2)t_{eff,TE}}, \quad (2)$$

where n_l is the real part of the refractive index of the adsorbed analyte, n_w is the refractive index of the alumina waveguiding film, n_c is the refractive index of the buffer solution, N_{TE} is the effective refractive index of the waveguide, $t_{eff,TE}$ is the effective thickness of the waveguide (which is related to physical thickness of the guiding film, t), and L is the distance between the input and output couplers. For the single-mode waveguide used in this work, the sensitivity factor is presented in Fig. 8 as a function of the wavelength for the spectral region of interest in this work. It is the extremely high value of the sensitive factor that makes possible the investigation of very low amounts of surface adsorbed species.

3.3 Determination of Surface Coverage and Kinetics of Chlorophyll a Adsorbed to Different Functionalized Surfaces

In order to calculate the surface density of chlorophyll *a*, we solved Eq. (1) for Γ

$$\Gamma = \frac{A_{WG,TE}}{S_{TE}\epsilon_{surf}}, \quad (3)$$

and used the experimental results of the peak absorbance, $A_{WG,TE}$, measured by our single-mode waveguide-based spectrometer and the results of the sensitivity factor, S_{TE} , from Eq. (2). In Fig. 9 we display the surface-adsorption kinetic results of chlorophyll *a* (surface density of chloro-

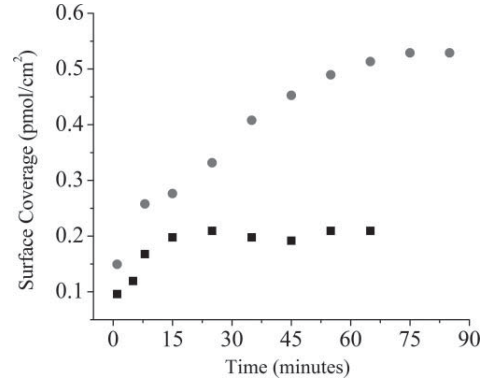


Fig. 9 Adsorption kinetics for chlorophyll *a* adsorbed onto the hydrophilic surface. In both cases, the amount of chlorophyll *a* dissolved in solution was the same ($1.4 \mu\text{M}$), as was the pH of the 7 mM sodium phosphate buffer (7.25). Black squares show that the concentration of NaCl was 1 mM; gray circles show that the concentration of NaCl was 10 mM.

phyll *a* versus time) onto the hydrophilic surface, and in Fig. 10 the corresponding results for the hydrophobic surface are shown. First, it is worth mentioning that the extremely high sensitivity of our single-mode integrated optical waveguide spectrometer allowed us to investigate surface concentrations as low as a few femtomoles-per- cm^2 . For the hydrophilic surface, the adsorption rate at initial times seems to be independent of the salt concentration, but for a higher salt concentration it takes longer to stabilize and it does so at a higher level of surface coverage. On the other hand, for the hydrophobic surface, the stabilization time seems to be independent of salt concentration, but a higher salt concentration drives a faster adsorption rate at initial times and a larger surface density of chlorophyll *a* when equilibrium is reached.

The experimental results of surface coverage for chlorophyll *a* adsorbed to different surfaces and dissolved in different buffer compositions are presented in Table 1; data of surface coverage correspond to values when the equilibrium has been reached. For a $1.4 \mu\text{M}$ solution of chlorophyll *a* dissolved in 7 mM of phosphate buffer, we obtained a surface density of $0.209 \text{ pmol}/\text{cm}^2$ for chlorophyll *a* adsorbed

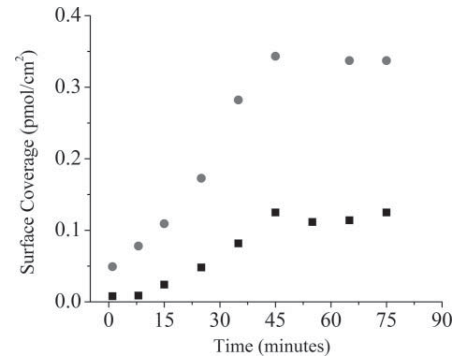


Fig. 10 Adsorption kinetics for chlorophyll *a* in contact to the hydrophobic surface. In both cases, the amount of chlorophyll *a* dissolved in solution was the same ($1.4 \mu\text{M}$), as was the pH of the 7 mM sodium phosphate buffer (7.25). Black squares show that the concentration of NaCl was 1 mM; gray circles show that the concentration of NaCl was 10 mM.

Table 1 Surface density for chlorophyll *a* adsorbed to different surfaces that was equally dissolved in solutions of phosphate buffer with different concentrations of sodium chloride.

Surface Composition	Surface Density for different buffer composition	
	7 mM sodium phosphate plus 1 mM sodium chloride	7 mM sodium phosphate plus 10 mM sodium chloride
178 nm aluminum oxide plus a monolayer of PEG Silane (hydrophilic)	0.209 pmol/cm ²	0.528 pmol/cm ²
178 nm aluminum oxide plus a monolayer of perfluorodecylsilane (hydrophobic)	0.125 pmol/cm ²	0.337 pmol/cm ²

to the hydrophilic PEG surface when the sodium chloride concentration was 1 mM. When the sodium chloride concentration was raised to 10 mM, the surface density increased to 0.528 pmol/cm². For a surface functionalized with a relatively more hydrophobic organic monolayer, the surface density of chlorophyll *a* adsorbed was 0.125 pmol/cm² for a sodium chloride concentration of 1 mM. When the concentration of sodium chloride was raised to 10 mM, the surface density of chlorophyll *a* increased to 0.337 pmol/cm². Therefore, our data show that increasing the concentration of sodium chloride in the dissolving solution dictates a higher surface density of chlorophyll *a*, regardless of the hydrophobicity of the surface. In addition, our data also shows that a higher surface density is reached for a hydrophilic surface indicating that chlorophyll *a* has a higher affinity to hydrophilic surfaces.

3.4 Molar Absorptivity of Chlorophyll *a* Adsorbed to Different Functionalized Surfaces

The molar absorptivity is generally a characteristic spectral fingerprint of a particular material mainly determined by the molecular structure. However, the nano-environment surrounding a particular molecule may affect its structures with possible consequences on the spectral profile of the molar absorptivity. For example, if a molecule is adsorbed to

a surface with a specific chemical composition and physical structure, the surface may perturb the spectroscopic properties of the pristine molecule. In addition, the composition of dissolved species in the solvent may also affect the optical properties of a particular analyte. To obtain the molar absorptivity for the adsorbed chlorophyll *a* across the entire spectral region available from our experimental data, we employed Eq. (1) and the results obtained in Secs. 3.2 and 3.3 for the waveguide sensitivity and surface density for each experiment. The results are presented in Fig. 11 for the hydrophilic surface and in Fig. 12 for the hydrophobic surface. In both Figs. 11 and 12 we have included the molar absorptivity of the dissolved species as obtained from data shown in Fig. 5. As previously mentioned, Fig. 5 clearly indicates that the increase of sodium chloride concentration in the solution from 1 to 10 mM does not affect the molar absorptivity of chlorophyll *a* in the dissolved phase. However, the results reported in Figs. 11 and 12 clearly demonstrate the dependence of chlorophyll *a* upon adsorption on both types of surfaces studied here. For the adsorbed molecules it generated a red-shift (5 nm on the hydrophobic surface and 15 nm on the hydrophilic surface) of the Soret band located at approximately 435 nm. A possible explanation for the observed red-shift of the Soret band at higher ionic strength of the bulk solvent is an aggregation of the chlorophyll *a* molecules. Red-shifted Soret bands have previously been observed for chlorophyll

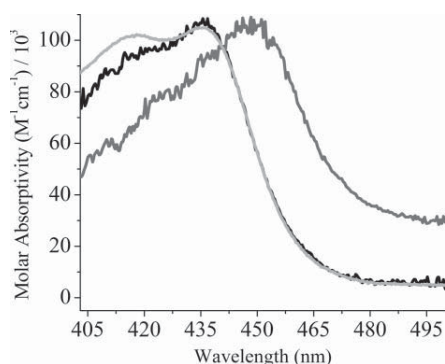


Fig. 11 Molar absorptivity of chlorophyll *a* adsorbed to hydrophilic surface. Black curve: surface-adsorbed chlorophyll *a* that was previously dissolved in 7 mM sodium phosphate buffer (pH 7.25), 1 mM sodium chloride; dark gray curve: surface-adsorbed chlorophyll *a* that was previously dissolved in 7 mM sodium phosphate buffer (pH 7.25), 10 mM sodium chloride; light gray curve: chlorophyll *a* in solution under the same conditions (obtained from a cuvette in a traditional spectrophotometer).

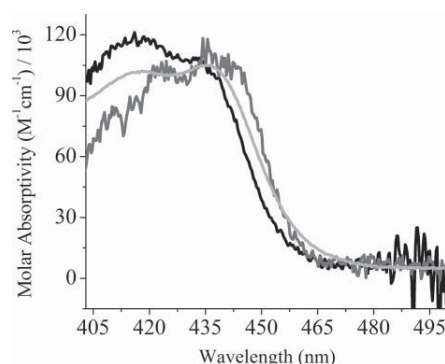


Fig. 12 Molar absorptivity of chlorophyll *a* adsorbed to hydrophobic surface. Black curve: surface-adsorbed chlorophyll *a* that was previously dissolved in 7 mM sodium phosphate buffer (pH 7.25), 1 mM sodium chloride; dark gray curve: surface-adsorbed chlorophyll *a* that was previously dissolved in 7 mM sodium phosphate buffer (pH 7.25), 10 mM sodium chloride; light gray curve: chlorophyll *a* in solution under the same conditions (obtained from a cuvette in a traditional spectrophotometer).

a dissolved in benzene and distributed as a thin liquid film upon a buffered aqueous subphase.²¹ Highly similar shifts of the Soret band have also been observed for chlorophyll dissolved in solutions of water-miscible organic solvents upon the addition of water to the organic solution.^{3,41} A wealth of experimental evidence supports aggregation of the pigment molecules in these solution studies.³ Aggregation in solutions have been attributed to a stronger hydrophobic effect between chlorophyll *a* molecules as the dielectric constant of the solvent is increased. Higher order aggregation of micellar chlorophyll *a* to polymeric forms has also been observed upon the addition of salt (KCl), accompanied by further redshifts in the absorption peaks.³ If the organic layer on the functionalized waveguide surfaces used in this study are behaving as a thin-film of liquid organic solvent, effectively dissolving both some water and chlorophyll *a* (or at least the phytol chain in the case of the hydrophobic surface), then an increase in the ionic strength of the buffer, which increases the polarity of the bulk solvent, might be expected to induce aggregation.

4 Summary and Conclusions

In this work we presented experimental results for the surface coverage and molar absorptivity of chlorophyll *a* adsorbed to hydrophilic and hydrophobic surfaces. This investigation was made possible by our single-mode, broadband, integrated optical waveguide spectrometer, which provides a highly sensitive tool that is able to measure absorbance at submonolayer levels of chlorophyll *a* in contact to a functionalized waveguide surface. Our experiments described here show that the surface composition and sodium chloride concentration in the dissolving solution play an important role in the surface coverage. In both surfaces we observed adsorption of chlorophyll *a*, however for the hydrophilic surface the surface coverage was higher. By increasing the concentration of sodium chloride in the dissolving solution we observed an increase in the absorbance and a red shift in the Soret peak for the hydrophilic surface-adsorbed chlorophyll *a*. The study of adsorption of chlorophyll *a* onto different surfaces presented herein can facilitate the design and understanding of emerging technologies inspired by biomolecular chromophores.

Acknowledgments

The authors acknowledge support from the National Institute of Health (NIH Grant No. RR022864) and National Science Foundation (NSF EPSCoR Grant No. 0814194) both awarded to SBM. We also thank Donald Yeager, Mark Crain, and Professor Kevin Walsh in the Micro/Nano Technology Center of University of Louisville for their support with the atomic and molecular layer deposition tools.

References

1. K. N. Ferreira, et al., "Architecture of the photosynthetic oxygen-evolving center," *Science* **303**, 1831–1838 (2004).
2. J. Yano, et al., "Where water is oxidized to dioxygen: structure of the photosynthetic Mn₄Ca cluster," *Science* **314**, 821–825 (2006).
3. A. Agostiano, et al., "Chlorophyll *a* behavior in aqueous solvents: formation of nanoscale self-assembled complexes," *J. Phys. Chem. B* **106**, 12820–12829 (2002).
4. L. L. Shipman, et al., "An analysis of the visible absorption spectrum of chlorophyll *a* monomer, dimer, and oligomers in solution," *J. Am. Chem. Soc.* **98**(25), 8222–8230 (1976).
5. P. Heathcote, P. K. Fyfe, and M. R. Jones, "Reaction centres: the structure and evolution of biological solar power," *Trends Biochem. Sci.* **27**(2), 79–87 (2002).

6. A. N. Melkozernov, J. Barber, and R. E. Blankenship, "Light harvesting in photosystem I supercomplexes," *Biochem. J.* **45**(2), 331–345 (2006).
7. R. Bassi, D. Sandona, and R. Croce, "Novel aspects of chlorophyll *a/b*—binding proteins," *Physiol. Plantarum* **100**, 769–779 (1997).
8. S. S. Brody and S. B. Brody, "Low temperature absorption spectra of chlorophyll *a* in polar and nonpolar solvents," *Biophys. J.* **8**, 1511–1533 (1968).
9. A. R. Wellburn, "The spectral determination of chlorophylls *a* and *b*, as well as total carotenoids, using various solvents with spectrophotometers of different resolution," *Plant Physiol.* **144**(3), 307–313 (1994).
10. S. B. Brody and S. S. Brody, "Emission spectra of chlorophyll *a* in polar and nonpolar solvents," *J. Chem. Phys.* **46**(9), 3334–3340 (1967).
11. T. J. Bensity, et al., "Observation of nanosecond laser induced fluorescence of *in vitro* seawater phytoplankton," *Appl. Opt.* **47**(22), 3980–3986 (2008).
12. D. F. Millie, et al., "Using absorbance and fluorescence spectra to discriminate microalgae," *European J. Phycol.* **37**, 313–322 (2002).
13. G. C. Papageorgiou and Govindjee, "Chlorophyll *a* fluorescence a signature of photosynthesis," in *Advances in Photosynthesis and Respiration*, Vol. 19, Springer-Verlag, New York (2004).
14. R. Steffen, G. Christen, and G. Renger, "Time-resolved monitoring of flash-induced changes of fluorescence quantum yield and decay of delayed light emission in oxygen-evolving photosynthetic organisms," *Biochemistry* **40**, 173–180 (2001).
15. Z. S. Kolber, O. Prasil, and P. G. Falkowski, "Measurements of variable chlorophyll fluorescence using fast repetition rate techniques: defining methodology and experimental protocols," *Biochim. Biophys. Acta* **1367**, 88–106 (1998).
16. X.-F. Wang, et al., "TiO₂ and ZnO based solar cells using a chlorophyll *a* derivative sensitizer for lightharvesting and energy conversion," *J. Photochem. Photobiol. A* **210**, 145–152 (2010).
17. Y. Amao and K. Kato, "Chlorophyll assembled electrode for photo-voltaic conversion device," *Electrochim. Acta* **53**, 42–45 (2007).
18. T. Itoh, et al., "Stabilization of chlorophyll *a* in mesoporous silica and its pore size dependence," *J. Mater. Chem.* **12**, 3275–3277 (2002).
19. S. Bousaad, A. Tazi, and R. M. Leblanc, "Chlorophyll *a* dimer: a possible primary electron donor for the photosystem II," *Proc. Natl. Acad. Sci. U.S.A.* **94**, 3504–3506 (1997).
20. C. Chapados, D. Germain, and R. M. Leblanc, "Aggregation of chlorophylls in monolayers. Part IV: The reorganization of chlorophyll *a* in multilayer array," *Biophys. Chem.* **12**, 189–198 (1980).
21. W. D. Bellamy, J. L. Gaines Jr., and A. G. Tweet, "Preparation and properties of monomolecular films of chlorophyll *a* and pheophytin *a*," *J. Chem. Phys.* **19**(10), 2528–2538 (1963).
22. S. Di Risio and N. Yan, "Adsorption and inactivation behavior of horseradish peroxidase on various substrates," *Colloids Surf. B* **79**, 397–402 (2010).
23. R. J. Green, I. Hopkinson, and R. A. L. Jones, "Unfolding and intermolecular association in globular proteins adsorbed at interfaces," *Langmuir* **15**, 5102–5110 (1999).
24. D. Song and D. Forciniti, "Effects of cosolvents and pH on protein adsorption on polystyrene latex: a dynamic light scattering study," *J. Colloid Interface Sci.* **221**(1), 25–37 (2000).
25. I. E. Araci, et al., "Highly sensitive spectroscopic detection of heme-protein submonolayer films by channel integrated optical waveguide," *Opt. Express* **15**(9), 5595–5603 (2007).
26. S. B. Mendes and S. S. Saavedra, "On probing molecular monolayers: a spectroscopic optical waveguide approach of ultra-sensitivity," *Opt. Express* **4**(11), 449–456 (1999).
27. K. Kato, et al., "A slab-optical-wave-guide absorption-spectroscopy of Langmuir-Blodgett-films with a white-light excitation source," *Chem. Lett.* **24**(6), 437–438 (1995).
28. S. B. Mendes, et al., "Broad-band attenuated total reflection spectroscopy of a hydrated protein film on a single mode planar waveguide," *Langmuir* **12**(14), 3374–3376 (1996).
29. J. T. Bradshaw, S. B. Mendes, and S. S. Saavedra, "A simplified broadband coupling approach applied to chemically robust sol-gel, planar integrated optical waveguides," *Anal. Chem.* **74**(8), 1751–1759 (2002).
30. S. B. Mendes and S. S. Saavedra, "Comparative analysis of absorbance calculations for integrated optical waveguide configurations by use of the ray optics model and the electromagnetic wave theory," *Appl. Opt.* **39**(4), 612–621 (2000).
31. M. B. Pereira, J. S. Craven, and S. B. Mendes, "A solid-immersion lens at aplanatic condition for enhancing the spectral bandwidth of a waveguide grating coupler," *Opt. Eng.* **49**, 124601 (2010).
32. M. M. Aslan, et al., "Low-loss optical waveguides for the near ultraviolet and visible spectral regions with Al₂O₃ thin films from atomic layer deposition," *Thin Solid Films* **518**(17), 4935–4940 (2010).
33. A. S. Anderson, et al., "Functional PEG-modified thin films for biological detection," *Langmuir* **24**(5), 2240–2247 (2008).
34. M. Doms, et al., "Hydrophobic coatings for MEMS applications," *J. Microchem. Microeng.* **18**, 055030 (2008).
35. R. S. Wiederkehr, et al., "Investigations on the Q and CT bands of cytochrome *c* submonolayer adsorbed on an alumina surface using

- broadband spectroscopy with single-mode integrated optical waveguides," *J. Phys. Chem. C* **113**, 8306–8312 (2009).
36. I. Tregub, et al., "Red-light-induced photoreactions of chlorophyll *a* mixtures with all-trans- or 9-cis- β -carotene," *J. Photochem. Photobiol. A* **98**(1–2), 51–58 (1996).
 37. C. M. Hayes, et al., "Sub-micron integrated grating couplers for single-mode planar optical waveguides," in *Proc. of 17th IEEE University Government Industry MicroNano Symposium (UGIM2008)*, pp. 227–232, IEEE, Piscataway, NJ (2008).
 38. M. Wanebo, et al., "Molecular vapor deposition (MVDTM)—a new method of applying moisture barriers for packaging applications," presented at *Intl. Symp. on Advantage Packaging Materials: Processes, Properties and Interfaces*, 16–18 March 2005, IEEE, Piscataway, NJ (2005).
 39. B. Kobrin, et al., "An improved chemical resistance and mechanical durability of hydrophobic FDTs coatings," *J. Phys.: Conf. Ser.* **34**, 454–457 (2006).
 40. W. P. Inskeep and P. R. Bloom, "Extinction coefficients of chlorophyll *a* and *b* in N,N-dimethylormamide and 80% acetone," *Plant Physiol.* **77**, 483–485 (1985).
 41. R. Vladkova, "Chlorophyll *a* self-assembly in polar solvent-water mixtures," *Photochem. Photobiol.* **71**(1), 71–83 (2000).



Rodrigo S. Wiederkehr received his BS degree in physics from University of Rio Grande do Sul, Brazil in 2003 and his PhD degree in applied physics from University of São Paulo, Brazil in 2007. Currently he is a post doc associate at the Department of Physics of the University of Louisville working with the development of new platforms for spectroscopic studies of monomolecular films deposited on different surfaces.



interests cover a range of biochemical topics from the molecular genetics of onion bulb color to folding of surface-adsorbed proteins.

Geoffrey C. Hoops received his BA in chemistry from Grinnell College (Grinnell, Iowa) in 1989 and his PhD degree in medicinal chemistry from the University of Michigan (Ann Arbor, Michigan) in 1995. Following a post-doctoral research under the supervision of Dr. V. Jo Davisson at Purdue University, he accepted a position in the Chemistry Department at Butler University (Indianapolis, Indiana) in 1999, where he is currently an associate professor. His teaching and research



Sergio B. Mendes received his bachelor degree in physics from the University of São Paulo, Brazil, in 1982. He then became a technical manager of Funbec, a private-foundation inside University of São Paulo focused on developing novel optical technologies in Brazil. In 1991, he went to the University of Arizona to pursue his PhD and got his degree in 1997 working under the supervision of Professor James Burke. Upon his graduation, he became a faculty member of the College of Optical Sciences at the University of Arizona, a position that he held until joining the University of Louisville in August 2006 as an associate professor in physics. From 2000 to 2003, he had a leave of absence from his academic appointment to be a director of NP Photonics Inc., a spin-off company created to develop novel optical fiber amplifiers and fiber lasers. His current research work at the University of Louisville focuses on the development and applications of integrated optic, guided-wave, and plasmonic technologies for research in biomolecular films and surface phenomena using several optical spectroscopic techniques. Mendes has been awarded with several research grants from agencies such as NSF, NIH, and NASA, has published more than 40 research articles in peer-reviewed journals, is the co-inventor of five licensed patents, has been invited for several talks at international conferences, has supervised and collaborated in the research project of several graduate and undergraduate students, and has served as a topical editor for the Journal Applied Optics of the Optical Society of America.